Increased efficacy of breast cancer chemotherapy in thrombocytopenic mice

Mélanie Demers[1,2], **Benoit Ho-Tin-Noé**[1,2,3], **Daphne Schatzberg**[1], **Janie J. Yang**[1], and **Denisa D. Wagner**[1,2]

[1] Immune Disease Institute, Boston, Massachusetts; the Program in Cellular and Molecular Medicine, Children's Hospital Boston, Boston, Massachusetts

[2] Department of Pathology, Harvard Medical School, Boston, Massachusetts

Abstract

Platelets contribute to homeostasis of the tumor vasculature by helping prevent hemorrhage. Thus, we hypothesized that inducing thrombocytopenia would increase tumor vascular leakiness and facilitate the effective delivery of chemotherapeutic agents to tumors. In a mammary carcinoma murine model, platelet depletion induced bleeding specifically at the tumor site, favoring the accumulation of fluorescently-labeled microspheres only in the tumor. Moreover, induction of thrombocytopenia in tumor-bearing mice before injection of paclitaxel increased its intratumoral accumulation and reduced growth of both slow- and fast-growing tumors, compared to mice with normal platelet counts that were treated only with paclitaxel. Histological analysis confirmed the expectation of an increase in tumor apoptosis and a reduction in tumor proliferation in thrombocytopenic mice receiving chemotherapy. No increased toxicity was seen in other organs or blood cells. Taken together, our results indicate that low platelet count selectively induces leakiness of tumor vessels and favors the delivery of chemotherapy to tumor sites, enhancing its tumoricidal effects.

Keywords

breast cancer; thrombocytopenia; hemorrhage; paclitaxel

Introduction

Cancer therapy is hampered by dose-limiting side effects that reduce the efficacy of cancer treatments. Conventional drugs used for treatment do not selectively accumulate in the tumor (1). Thus, important research goals include delivering high doses of drug to tumor sites for maximum treatment efficacy while minimizing side effects to healthy tissues (2). In the search for more effective treatments, efforts are made to develop drugs that selectively target tumor antigens to preferentially deliver the therapeutic agent to the tumor site (1,3). Antigen heterogeneity among diverse types of tumors, and among tumor cells of the same tumor, renders this approach effective only in specific cases.

Other strategies target tumoral neovasculature. Angiogenesis is a hallmark feature of cancer growth and tumor vessels in distinct tumors may also express markers that are different from

normal vasculature (4). The targeting of angiogenesis is therefore applicable to a wide range of different tumors. Antibodies targeting VEGF, PDGF, and integrins have been described and used to alter tumor vessels in animal and clinical studies (5-8). Unfortunately, anti-angiogenic therapies in cancer have until now shown only limited or transient effects (9-11).

Platelets are a rich source of pro- and anti-angiogenic factors that are released in the circulation upon platelet activation (12). Platelets also maintain the integrity of angiogenic and inflamed microvessels (13,14). Furthermore, we recently showed that platelets support tumor vascular homeostasis by preventing intratumoral hemorrhaging (15). The tumor bleeding induced by thrombocytopenia cannot be prevented by degranulated platelets suggesting that the local release of soluble factors protects the tumor endothelium against injuries produced by tumor-associated inflammatory cells (15,16).

Because thrombocytopenia renders vessels in the tumor leaky, we hypothesized that this leakiness would enhance the access of chemotherapy to the tumor. Paclitaxel is a well-known therapeutic drug used to treat breast cancer. It acts as a mitotic inhibitor that stabilizes microtubules, interfering with their normal breakdown during cell division inducing apoptosis (17-19). Here we show that thrombocytopenia promotes the accumulation of inert particles at the tumor site reflecting an increase in porosity of the tumor vessels. Using mammary and lung carcinoma mouse models, we show that thrombocytopenia enhances the inhibitory effect of paclitaxel on tumor growth without increasing its toxicity to other organs.

Materials and Methods

Cell lines and reagents

The 4T1 and LLC cell lines were maintained in high glucose Dulbecco's Modified Eagle Medium (DMEM) + L-GlutaMAX-1 [supplemented with 10% (v/v) FCS, 10 mmol/L HEPES buffer, 10 mmol/L sodium carbonate (4T1 cells)]. The 4T1 cell line was originally isolated from a spontaneously arising mammary tumor in a BALB/c mouse (20) whereas LLC cells originated from C57BL/6 mice. The 4T1 and LLC cells were injected in syngeneic mice after less than 4 and 10 serial passages in vitro respectively. For the fast-growing 4T1 model, the cells were cultivated for over 25 passages. All cell lines were obtained from and characterized by ATCC according to the cell line authentification testing (growth curve analysis, mycoplasma, bacteria, and fungi contamination, DNA profiling, species confirmation) and were used within 6 months after resuscitation. All cell culture products were purchased from Life Technologies/Invitrogen.

Animals

All animal procedures described in this study were performed using 6- to 8-wk-old BALB/c female mice or C57BL/6 males (purchased from The Jackson Laboratory) except in experiments using dorsal skinfold chamber for which 10-wk-old mice were used. All experimental procedures involving the use of mice were approved by the Animal Care and Use Committee of the Immune Disease Institute.

Induction of thrombocytopenia

Thrombocytopenia was induced by an i.v. injection of 2.5 μg/g of a platelet depleting antibody (polyclonal rat IgG anti-mouse GPIbα; emfret Analytics). Control mice were injected with a non-immune rat polyclonal IgG (emfret Analytics). Thrombocytopenia was verified by flow cytometry and resulted in less than 5% of normal platelet count.

Determination of hemoglobin content

Organs and tumors of sacrificed animals were excised, weighed, homogenized in Drabkin's reagent (Sigma), and centrifuged ($2000 \times g$; 10 min). Hemoglobin content of supernatants was measured by absorbance at 540 nm.

Immunohistology

Tumors and organs were harvested from sacrificed animals and fixed in zinc fixative (100 mmol/L Tris-HCl containing 37 mmol/L zinc chloride, 23 mmol/L zinc acetate, and 3.2 mmol/L calcium acetate). Paraffin-embedded sections were deparaffinized in xylenes and rehydrated through a graded alcohol series. For Perl's Prussian blue staining, the sections were transfered to a mixture of equal parts of 2% potassium ferrocyanide and 2% hydrochloric acid. Sections were counterstained with nuclear fast red. Tissues were dehydrated, mounted in DPX mountant (Fluka BioChemika) and observed by light microscopy. For quantification of apoptosis, the sections were permeabilised and stained with terminal deoxynucleotidyl transferase-mediated dUTP nick end labeling (TUNEL; Roche Applied Science) according to the manufacturer's instructions. For quantification of proliferation, the sections were stained with Ki-67-Alexa 555 conjugated antibody (BD Biosciences). For quantification of apoptotic endothelial cells, the sections were stained with TUNEL as described above, incubated with a rat anti-CD31 antibody (eBioscience) and anti-rat Alexa-594 (Invitrogen) as secondary antibody. The percentage of apoptotic cells was determined as the ratio of TUNEL-positive nuclei of CD31-positive cells to the total CD31-positive cells. Pericytes were stained using a rabbit anti-NG2 antibody (Chemicon) followed by incubation with an anti-rabbit Alexa-488 (Invitrogen). Sections were counterstained with Hoechst to visualize all nuclei, mounted with Fluoro-gel (Electron Microscopy Sciences) and observed under an epifluorescent microscope.

Imaging of fluorescently labeled microspheres

Dorsal skinfold chambers and surgical preparation were performed as described (21). After 2 days recovery, 1×10^6 4T1 or LLC cells were implanted in the conjunctive tissue below the striated skin muscle layer and allowed to grow for 5 days. Thrombocytopenia was induced and mice were then injected i.v. with 100×10^6 1μm FluoSpheres, red fluorescent carboxylate-modified microspheres (Invitrogen) 5 min later. Tumors were photographed 24 hours after injection of the platelet depleting or control antibody. Microscopy imaging was performed using an upright microscope (Axioplan; Zeiss) with X 2.5 or X 4 magnification objectives and recorded by attached digital camera (AxioCam HRc).

Induction of tumors and chemotherapeutic treatments

4T1 cells (4×10^5) were inoculated in the mammary fat-pad of 6-8 wk-old BALB/c mice. For the LLC model, 1.5×10^6 cells were inoculated subcutaneously in the right flank of 6-8 week-old C57BL/6 mice. Animals were monitored twice a week at which time tumors were carefully measured using calipers. The tumor volume was calculated using the formula $V = lw^2 \times 0.4$ where l is the length and w the width (22). For chemotherapeutic treatment, tumor-bearing mice were randomly distributed into four groups and injected i.v. with either the platelet depleting or control antibody. Three hours later, mice were injected i.p. with paclitaxel (30mg/kg) (Sigma) (Cremophor EL:Ethanol; 1:1 diluted in PBS) or vehicle. For treatment characterization 72 hours post-treatment, blood was collected and analyzed using the Hemavet blood cell counter (Drew Scientific, Inc.). Tumor, spleen, liver and kidneys were examined and collected at necropsy.

Quantification of radiolabeled-paclitaxel in the mammary tumor

At day 10 after injection of 4T1 cells, the mice were randomly distributed into two groups and injected i.v. with either the platelet depleting or control antibody. Three hours later, mice were injected i.v. with ^{3}H-paclitaxel (5μCi/20g mouse) (Moravek Biochemicals Inc.) and sacrificed after two hours. The tumors were collected, weighed, and solubilized in Solvable (Perkin Elmer) overnight at 60°C, treated with hydroxyperoxide 30% (Sigma), and analyzed for radioactivity by liquid scintillation counting in a TRI-CARB liquid scintillation analyzer (Perkin Elmer).

LDH activity of tumor homogenate

For quantification of necrosis, the tumors were harvested and assessed for LDH activity using the Quantichrom Lactate Dehydrogenase Kit (BioAssay Systems) according to the manufacturer's instructions.

Statistical analysis

Data are represented as mean ± SEM and were analyzed by a two sided Kruskal-Wallis test to compare more than three groups. Two-sided Mann Whitney test was performed between groups at each time point. All p-values were considered significant at the 0.05 level.

Results

Acute thrombocytopenia induces bleeding only at the tumor site

We previously showed that thrombocytopenia induces tumor hemorrhage without any macroscopic signs of bleeding in other organs (15). To address this more precisely, we determined the hemoglobin content, reflecting the level of red blood cell extravasation, of the major organs in thrombocytopenic versus control tumor-bearing mice. For this purpose, 4T1 mammary carcinoma cells were implanted in the mammary fat pad of BALB/c syngeneic mice and allowed to grow. At day 8, platelet depletion was induced for 24 hours; subsequently mice were sacrificed and the hemoglobin content of the organs and tumor was quantified. The hemoglobin content in the tumors of mice with normal platelet count was similar to that of the skin and less than that of highly vascularized organs such as lung, liver, and heart as expected (23). No significant difference in the hemoglobin content of major organs was found between thrombocytopenic mice and controls (Figure 1A). In contrast, a significant increase in hemoglobin content and the presence of extravasated red blood cells (Figure 1B) were observed in mammary carcinomas of thrombocytopenic mice compared to mice with normal platelet count. Furthermore, histopathological analysis of paraffin-embedded tissues revealed no extravasated red blood cells (yellow/brown) nor positive staining for ferric iron/hemosiderin (blue) in the major organs except in the spleen of both control and thrombocytopenic mice (Supplementary Figure 1). These results show that platelet depletion in tumor-bearing mice induces red blood cell leakage specifically in the tumoral vasculature, while intact vasculature is maintained in other organs.

To determine the status of tumor vessels 24 hours after induction of thrombocytopenia, we evaluated the percentage of apoptotic endothelial cells in the tumors of thrombocytopenic mice compared to control mice. Immunostaining analysis revealed a similar frequency of apoptotic endothelial cells in the vessels (Figure 1C). No obvious differences in the mean diameter of the tumor vessels (Control 8.0 ± 1.1 μm vs. Depleted 8.0 ± 0.2 μm; p>0.05, n=3) and in the number of NG2-positive pericytes within the tumor sections (Control 419.9 ± 30.1 pericytes/mm^2 vs. Depleted 473.8 ± 22.4 pericytes/mm^2; p>0.05, n=4) were observed. These results indicate that the overall structure of tumor vessels is maintained during acute thrombocytopenia and that the thrombocytopenia-induced hemorrhage is not a result of apoptosis of endothelial cells or loss of pericytes around tumor vessels.

Thrombocytopenia induces tumor vascular porosity that allows accumulation of fluorescently labeled microspheres

Knowing that the absence of platelets induces tumor hemorrhage, we hypothesized that thrombocytopenia results in the formation of breaches in the tumor vasculature through which circulating particles could pass. To investigate whether tumor hemorrhage induces accumulation of circulating particles at the tumor site, we implanted 4T1 cells in dorsal skinfold window chambers placed on the backs of BALB/c mice. Induction of thrombocytopenia in such mice bearing a 5-day-old tumor in the skinfold results in tumor hemorrhage (Figure 2A). Five minutes after platelet depletion we injected 1μm fluorescently labeled microspheres into the bloodstream. Intravital observation of the tumor through the dorsal skinfold chamber revealed a massive deposition of fluorescent microbeads at the site of hemorrhage 24 hours after platelet depletion (Figure 2 B,C). The microspheres concentrated particularly in the vicinity of hemorrhaging blood vessels. This accumulation of microspheres was seen in all five tumors of thrombocytopenic mice whereas no accumulation was observed in four tumors in mice with normal platelet count. This result indicates that the selective induction of tumor hemorrhage by platelet depletion facilitates the delivery and accumulation of circulating particles to the tumor site, likely through openings in the vasculature that also allow the red blood cell extravasation.

Porosity of tumor vessels induced by thrombocytopenia enhances the effect of paclitaxel on mammary tumors

The capacity of acute thrombocytopenia to favor the intratumoral accumulation of microbeads suggests that short term platelet depletion could improve the inhibitory effect of paclitaxel on tumor growth. Therefore, we evaluated the effect of paclitaxel treatment combined with acute thrombocytopenia on the growth of slow- and fast-growing tumors. Mammary tumor 4T1 cells cultivated for less than 4 *in vitro* passages (Figure 3A; slow-growing tumors) or for over 25 *in vitro* passages (Figure 3B; fast-growing tumors) were allowed to grow in BALB/c mice. When the tumors reached 50-100mm^3, the mice were infused intravenously with the platelet depleting or control antibody and 2-3 hours later were injected intraperitoneally with paclitaxel or vehicle and tumor growth was measured after 3 and 8 days (Figure 3). At day 11, three days after the injections, a significant reduction in tumor growth of both the slow- and the fast-growing tumors was observed in the group of mice that received both treatments compared to paclitaxel alone, platelet depletion alone, or control mice. At day 16, 8 days after the injections, an average 20% reduction in growth of the slow-growing tumors (2.782 ± 0.1873 versus 3.464 ± 0.3789) and 27% reduction in growth of the fast-growing tumors (4.069 ± 0.3702 versus 5.585 ± 0.2579) were observed in mice that received both treatments compared to control mice. This reduction was only significant in the fast-growing tumors where paclitaxel, affecting dividing cells, may have had access to more targets. These results suggest that thrombocytopenia enhances the delivery of paclitaxel to the tumor site and improves its tumoricidal effects.

Acute thrombocytopenia increases delivery of paclitaxel to tumors

To evaluate if the reduction in tumor growth observed in combination treatments was the result of an increase in the delivery of drug to the hemorrhagic tumors, we quantified the presence of radiolabeled-paclitaxel in mammary tumors of thrombocytopenic mice compared to mice with normal platelet count. Mice bearing 10 day-old tumors were treated with either the platelet depleting or control antibody and injected 3 hours later with ^{3}H-paclitaxel. Quantification of the radioactivity in the hemorrhagic tumors revealed a significant increase of paclitaxel in the tumors of thrombocytopenic mice compared to control tumors of similar size. (Figure 4A, B). Thrombocytopenia-induced tumor bleeding results in the accumulation of about 40% more radio-labeled drug in the thrombocytopenic

tumors compared to controls. This result shows that by inducing tumor bleeding acute thrombocytopenia allows the accumulation of circulating chemotherapeutic drug in tumors.

Increased apoptosis and reduced proliferation in mammary tumors of thrombocytopenic mice treated with paclitaxel

To determine whether the observed reduction in tumor growth was characterized by the known actions of paclitaxel, we compared the effect of the drug on tumor cell apoptosis and proliferation 72 hours post-treatments. Immunofluorescent analysis revealed a significant increase in the number of apoptotic cells (Figure 4C) and a significant reduction in the number of proliferative cells (Figure 4D) in the tumors of mice that received both treatments. No significant change in necrosis was seen in the thrombocytopenic tumors as assessed by LDH activity of the tumor homogenate (vehicle treated 4246 ± 762 IU/L and paclitaxel treated 3761 ± 132 IU/L) compared to their respective normal platelet count controls (vehicle treated 3747 ± 772 and paclitaxel treated 4010 ± 288 IU/L). These results indicate that the observed change in rate of tumor growth in thrombocytopenic mice reflects the expected effects of paclitaxel. Taken together, the results indicate that thrombocytopenia, by increasing the leakiness of tumor vessels, improves presentation of the drug to the tumor, allowing it to further affect the tumor.

Thrombocytopenia does not increase the overall toxicity of chemotherapeutic treatment

Chemotherapeutic treatments are known to display a wide range of side effects (24). To determine whether the absence of platelets also has an impact on the unspecific toxicity of paclitaxel treatment, we evaluated apoptosis in the liver, kidneys, and spleen in tumor-bearing mice three days after treatment. The results showed that while injection of either the vehicle or paclitaxel increased apoptosis in the liver and kidney (Figure 5), no additional significant increase was observed in mice treated with the platelet depleting antibody. No signs of apoptosis were seen in the spleen in any of the groups (not shown).

Cell counter analysis of blood samples collected three days after the mice received combined treatments revealed a persistent significant reduction in platelet count but no significant differences in the number of white blood cells and red blood cells compared to the other groups (Figure 6). Although not significant, thrombocytopenic mice showed a tendency toward reduced number of red blood cells. This reduction could be explained by the tumor hemorrhage occurring in these mice. Altogether our results indicate that by depleting platelets and rendering leaky only the vessels of the tumor, we enhanced the access of chemotherapy to the tumor site specifically and did not increase its general toxicity.

Thrombocytopenia allows accumulation of microspheres and enhances the effect of paclitaxel on Lewis lung carcinoma (LLC) tumor growth

We previously showed that thrombocytopenia-induced tumor hemorrhage was independent of the type, age, and localization of the tumor (15). To examine whether increased drug delivery to tumors in thrombocytopenic mice could be generalized to other tumors, we studied LLC inoculated into the flank of syngeneic mice. First, we evaluated if thrombocytopenia-induced tumor hemorrhage in this model allows the accumulation of circulating particles at the tumor site. Indeed, fluorescently-labeled microspheres accumulated preferentially in the hemorrhagic compared to the non-hemorrhagic tumors (Figure 7A). Moreover, the combined treatment of platelet depletion and paclitaxel injection also resulted in a significant reduction of LLC tumor growth compared to treatment with paclitaxel alone. (Figure 7B). These results indicate that low platelet counts can be used to increase the delivery and efficacy of a chemotherapeutic agent to different types of tumors.

Discussion

Selective induction of tumor hemorrhage by targeting platelet function may facilitate the delivery of chemotherapeutic agents to tumors. This hypothesis is supported by the following observations: (a) thrombocytopenia induces tumor bleeding without detectable hemorrhaging elsewhere, (b) the absence of platelets induced porosity of tumor vessels favoring the accumulation of inert particles in the tumor, and (c) the combination of thrombocytopenia with a chemotherapeutic treatment increased the delivery and enhanced the effect of the drug on tumor growth and viability without increasing toxicity to other organs. The present study follows previous publications from our group showing that platelets prevent bleeding of angiogenic vessels (13) and continuously prevent intratumoral hemorrhage induced by tumor infiltrating inflammatory cells by the secretion of their granule contents (15,16). Given that all tumors are both angiogenic and pro-inflammatory (25,26), we now show that the thrombocytopenia-induced leakiness of tumor vessels allows better access of a chemotherapeutic agent to the tumor, thus increasing its efficacy.

An important goal in cancer therapy is to deliver high doses of drug to tumor sites while minimizing side effects to healthy organs. Conventional drugs used for cancer treatment are administered systemically and distribute within the different organs and tissues of the body. The dose that reaches the tumor mass may be as little as 5-10% of that which accumulates elsewhere (27). Therapies that target specific tumor antigens are limited by their specificity and may not be possible to develop for cancers that are not well-defined.

Our model of thrombocytopenia induction favors the accumulation of particles and drug in bleeding tumors without targeting a particular antigen. We also demonstrate that thrombocytopenia in combination with the chemotherapeutic treatment significantly reduced growth of two different tumor types. The vascular damage caused by thrombocytopenia is due to the tumor's inflammatory cells: neutrophils and monocytes (16). Since inflammatory cells are present in all tumors (28), inhibition of platelet function to improve drug delivery should be widely applicable.

Mouse models of disease treatment are not always directly applicable to human patients. In fact, the use of thrombocytopenia to improve chemotherapeutic treatment could raise concerns for the well-being of patients. However, we showed here that no signs of systemic hemorrhage were associated with thrombocytopenia. Moreover, low platelet counts needed to be achieved only transiently to be effective in our model. We previously showed that commencement of tumor hemorrhage can be seen as soon as 30 minutes after the induction of thrombocytopenia (15). Perhaps thrombocytopenia would only need to occur long enough to induce tumor hemorrhage and allow drug accumulation. It must also be noted that chemotherapeutic agents are characterized by a short half-life. Maintaining thrombocytopenia in patients for more than a few hours would therefore not increase the effect of the drug. Once the drug is no longer in circulation, normal platelet counts should be restored. In addition, chemotherapies are themselves known to induce thrombocytopenia in patients (29,30). Treatment schedules could be adjusted to take advantage of the already occurring thrombocytopenia-induced injuries of tumor vessels to enhance drug delivery by delaying platelet transfusion.

Platelets are key players in tumor vascular homeostasis. More than 300 proteins and small molecules have been shown to be secreted from activated platelets (31). It is known that bleeding cannot be prevented by degranulated platelets, suggesting that platelet granule contents are important to arrest bleeding in the tumor by the local release of soluble factors that heal or prevent inflammatory injuries (15,16). Platelet granules are known to contain both pro- and anti-angiogenic factors, cytokines, chemokines, growth factors, and many

other molecules that could potentially influence vessel injuries. Since the 1990's, platelet releasate has been used to heal wounds and autologous platelet-rich plasma has been shown to protect against capillary bleeding (32). To our knowledge, the factor(s) responsible for this particular function of platelets are still unknown and are currently under investigation in our laboratory. Identification of these factor(s) responsible for the prevention of bleeding would open a new area of drug development. Potentially, physicians may target platelets' ability to prevent tumoral hemorrhage specifically without inducing thrombocytopenia. Such anti-platelet treatment combined with chemotherapy to enhance drug delivery to the tumor would represent a significant improvement in our ability to fight cancer with minimal side effects.

Supplementary Material

Refer to Web version on PubMed Central for supplementary material.

Acknowledgments

References

1. Schliemann C, Neri D. Antibody-based targeting of the tumor vasculature. Biochim Biophys Acta. 2007; 1776:175–92. [PubMed: 17920773]

2. Langer R. Drug delivery and targeting. Nature. 1998; 392:5–10. [PubMed: 9579855]

3. Peer D, Karp JM, Hong S, Farokhzad OC, Margalit R, Langer R. Nanocarriers as an emerging platform for cancer therapy. Nat Nanotechnol. 2007; 2:751–60. [PubMed: 18654426]

4. St Croix B, Rago C, Velculescu V, et al. Genes expressed in human tumor endothelium. Science. 2000; 289:1197–202. [PubMed: 10947988]

5. Ferrara N, Hillan KJ, Gerber HP, Novotny W. Discovery and development of bevacizumab, an anti-VEGF antibody for treating cancer. Nat Rev Drug Discov. 2004; 3:391–400. [PubMed: 15136787]

6. Klosowska-Wardega A, Hasumi Y, Burmakin M, et al. Combined anti-angiogenic therapy targeting PDGF and VEGF receptors lowers the interstitial fluid pressure in a murine experimental carcinoma. PLoS One. 2009; 4:e8149. [PubMed: 19997591]

7. Gutheil JC, Campbell TN, Pierce PR, et al. Targeted antiangiogenic therapy for cancer using Vitaxin: a humanized monoclonal antibody to the integrin alphavbeta3. Clin Cancer Res. 2000; 6:3056–61. [PubMed: 10955784]

8. McNeel DG, Eickhoff J, Lee FT, et al. Phase I trial of a monoclonal antibody specific for alphavbeta3 integrin (MEDI-522) in patients with advanced malignancies, including an assessment of effect on tumor perfusion. Clin Cancer Res. 2005; 11:7851–60. [PubMed: 16278408]

9. Bergers G, Hanahan D. Modes of resistance to anti-angiogenic therapy. Nat Rev Cancer. 2008; 8:592–603. [PubMed: 18650835]

10. Ebos JM, Lee CR, Kerbel RS. Tumor and host-mediated pathways of resistance and disease progression in response to antiangiogenic therapy. Clin Cancer Res. 2009; 15:5020–5. [PubMed: 19671869]

11. Grothey A, Galanis E. Targeting angiogenesis: progress with anti-VEGF treatment with large molecules. Nat Rev Clin Oncol. 2009; 6:507–18. [PubMed: 19636328]

12. Italiano JE Jr. Richardson JL, Patel-Hett S, et al. Angiogenesis is regulated by a novel mechanism: pro- and antiangiogenic proteins are organized into separate platelet alpha granules and differentially released. Blood. 2008; 111:1227–33. [PubMed: 17962514]

13. Kisucka J, Butterfield CE, Duda DG, et al. Platelets and platelet adhesion support angiogenesis while preventing excessive hemorrhage. Proc Natl Acad Sci U S A. 2006; 103:855–60. [PubMed: 16418262]

14. Goerge T, Ho-Tin-Noe B, Carbo C, et al. Inflammation induces hemorrhage in thrombocytopenia. Blood. 2008; 111:4958–64. [PubMed: 18256319]

15. Ho-Tin-Noe B, Goerge T, Cifuni SM, Duerschmied D, Wagner DD. Platelet granule secretion continuously prevents intratumor hemorrhage. Cancer Res. 2008; 68:6851–8. [PubMed: 18701510]

16. Ho-Tin-Noe B, Carbo C, Demers M, Cifuni SM, Goerge T, Wagner DD. Innate immune cells induce hemorrhage in tumors during thrombocytopenia. Am J Pathol. 2009; 175:1699–708. [PubMed: 19729481]

17. Rowinsky EK, Donehower RC. Paclitaxel (taxol). N Engl J Med. 1995; 332:1004–14. [PubMed: 7885406]

18. Wieder T, Essmann F, Prokop A, et al. Activation of caspase-8 in drug-induced apoptosis of B-lymphoid cells is independent of CD95/Fas receptor-ligand interaction and occurs downstream of caspase-3. Blood. 2001; 97:1378–87. [PubMed: 11222383]

19. Park SJ, Wu CH, Gordon JD, Zhong X, Emami A, Safa AR. Taxol induces caspase-10-dependent apoptosis. J Biol Chem. 2004; 279:51057–67. [PubMed: 15452117]

20. Aslakson CJ, Miller FR. Selective events in the metastatic process defined by analysis of the sequential dissemination of subpopulations of a mouse mammary tumor. Cancer Res. 1992; 52:1399–405. [PubMed: 1540948]

21. Leunig M, Yuan F, Menger MD, et al. Angiogenesis, microvascular architecture, microhemodynamics, and interstitial fluid pressure during early growth of human adenocarcinoma LS174T in SCID mice. Cancer Res. 1992; 52:6553–60. [PubMed: 1384965]

22. Attia MA, Weiss DW. Immunology of spontaneous mammary carcinomas in mice. V. Acquired tumor resistance and enhancement in strain A mice infected with mammary tumor virus. Cancer Res. 1966; 26:1787–800. [PubMed: 4288553]

23. Langley RR, Russell J, Eppihimer MJ, et al. Quantification of murine endothelial cell adhesion molecules in solid tumors. Am J Physiol. 1999; 277:H1156–66. [PubMed: 10484438]

24. Tipton, JM. Handbook of Cancer Chemotherapy. Lippincott Williams & Wilkins; Philadelphia: 2003. Side effects of cancer chemotherapy.; p. 561-80.

25. Hanahan D, Weinberg RA. The hallmarks of cancer. Cell. 2000; 100:57–70. [PubMed: 10647931]

26. Coussens LM, Werb Z. Inflammation and cancer. Nature. 2002; 420:860–7. [PubMed: 12490959]

27. Bosslet K, Straub R, Blumrich M, et al. Elucidation of the mechanism enabling tumor selective prodrug monotherapy. Cancer Res. 1998; 58:1195–201. [PubMed: 9515805]

28. Grivennikov SI, Greten FR, Karin M. Immunity, inflammation, and cancer. Cell. 2010; 140:883–99. [PubMed: 20303878]

29. Benjamin RJ, Anderson KC. What is the proper threshold for platelet transfusion in patients with chemotherapy-induced thrombocytopenia? Crit Rev Oncol Hematol. 2002; 42:163–71. [PubMed: 12007974]

30. Vadhan-Raj S. Management of chemotherapy-induced thrombocytopenia: current status of thrombopoietic agents. Semin Hematol. 2009; 46:S26–32. [PubMed: 19245931]

31. Coppinger JA, Cagney G, Toomey S, et al. Characterization of the proteins released from activated platelets leads to localization of novel platelet proteins in human atherosclerotic lesions. Blood. 2004; 103:2096–104. [PubMed: 14630798]

32. Anitua E, Andia I, Ardanza B, Nurden P, Nurden AT. Autologous platelets as a source of proteins for healing and tissue regeneration. Thromb Haemost. 2004; 91:4–15. [PubMed: 14691563]

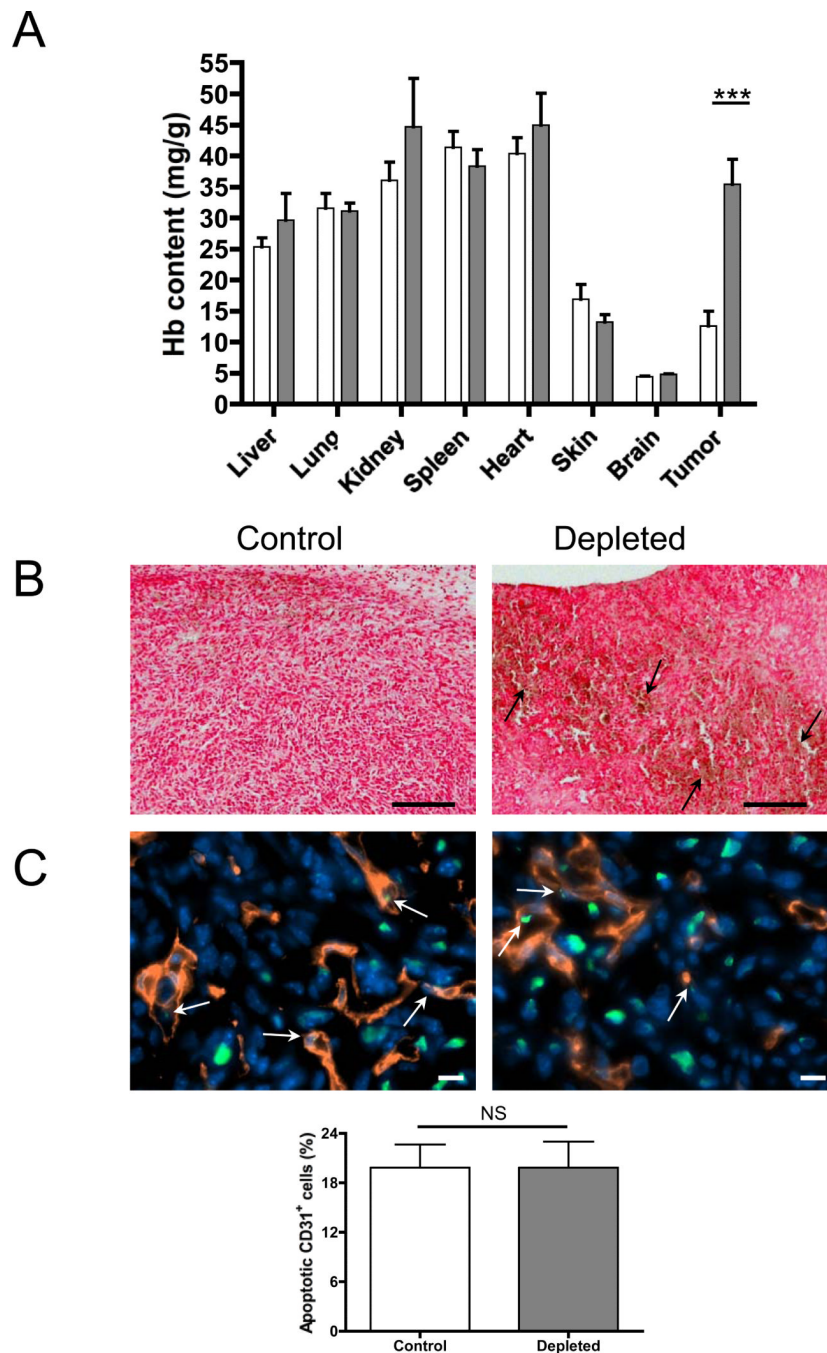**Figure 1. Acute thrombocytopenia induces bleeding only at the tumor site**

A, Hemoglobin content of organs and tumors of mice that have been treated with platelet depleting antibody (grey bars) or control antibody (white bars) for 24h. Mice were sacrificed, the organs and mammary tumors were harvested and the hemoglobin content was determined (n=4 mice; ***p≤0.001). B, Histopathological analysis of the tumors of thrombocytopenic mice (Depleted) or control mice (Control). Tissues were fixed and stained with the Perl's Prussian blue method. Blue=hemosiderin (no blue stain was observed), red=tissues and nuclei and yellow/brown=erythrocytes (arrows). Original magnification 100X, Bar = 200µm. C, Immunostaining analysis and quantification of apoptotic endothelial cells (arrows) of the tumors of platelet-depleted or control mice using anti-CD31 and

TUNEL labeling. Green=TUNEL, red=anti-CD31, blue=Hoechst. Original magnification 630X, Bar = 10μm. Bar graph shows the mean percentage of apoptotic CD31+ cells calculated from 6 microscopic fields of each tumor (n=4 mice; p>0.05; NS).
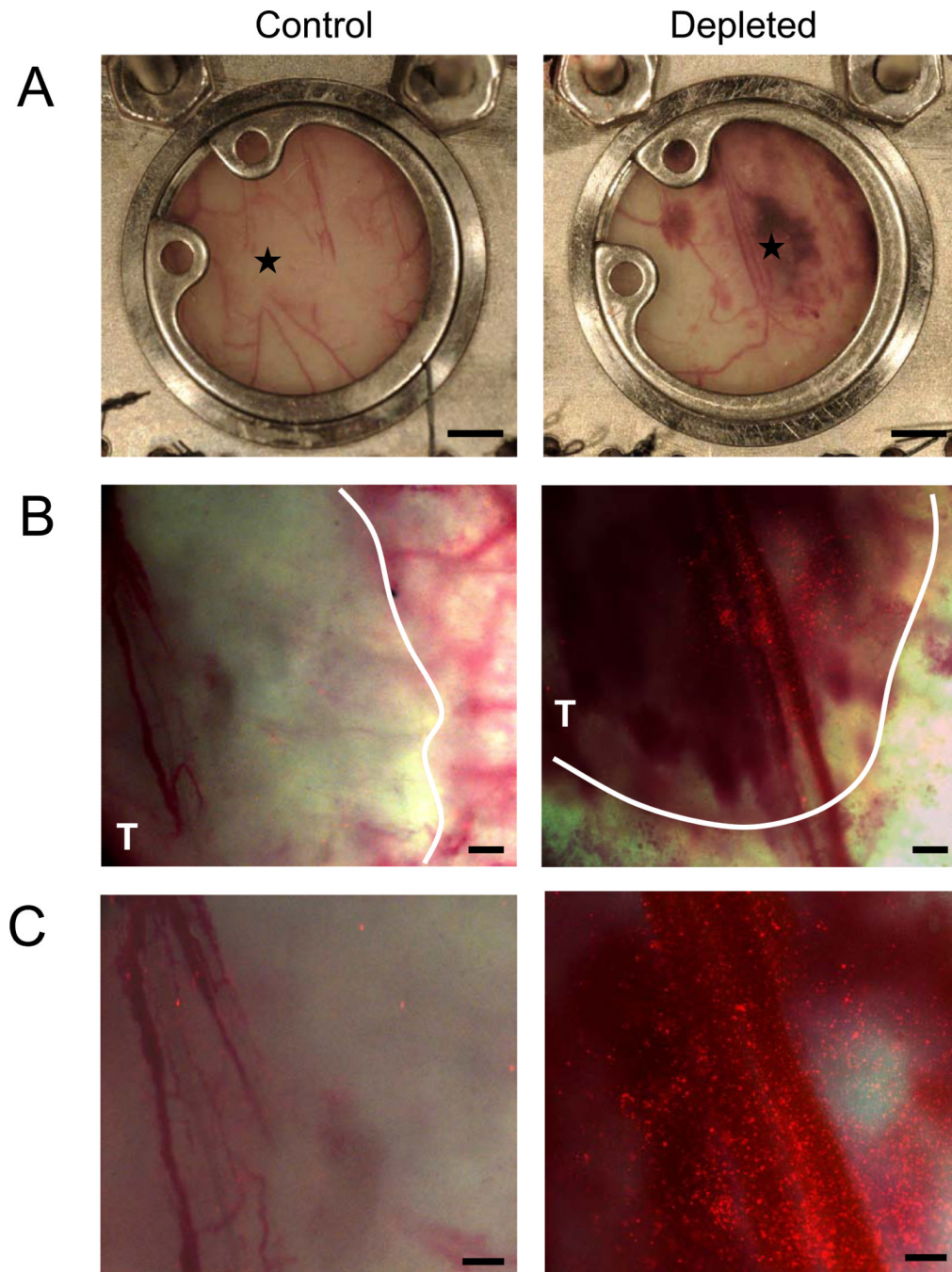
Figure 2. Tumor hemorrhage caused by acute thrombocytopenia favors the accumulation of fluorescently labeled microspheres

Dorsal skinfold chambers were surgically implanted on the backs of mice. Two days later, 4T1 tumor cells were injected within skinfold chamber and allowed to grow for 5 days. A, Photographs of the tumors were taken 24 hours after mice were injected with either a control antibody (Control) or a platelet depleting antibody (Depleted). Five minutes after injection of either control or platelet depleting antibody, 100×10^6 1μm fluorescent microspheres were injected into all mice. B,C, Images of a control and a thrombocytopenic tumor were taken at 25X (B) and at 40X (C) magnification. Results are representative of 5 different

hemorrhagic tumors and 4 non-hemorrhagic tumors. (A) Bar = 2mm; (B) Bar = 400μm; (C) Bar = 200μm. ★ = center of the tumor. T = tumor delineated by a white line.
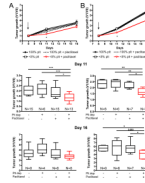
Figure 3. Injection of paclitaxel following thrombocytopenia significantly reduces mammary tumor growth

Tumor-bearing mice were treated on day 8 (arrow) as indicated and tumor growth was monitored. A, Tumor growth, after injection of 4T1 cells cultured less than 4 passages *in vitro*, represented as the ratio of the tumor volume at a specific day (V1) to the tumor volume before treatment (V0). B, Same analysis of tumor growth using long-term serial culture passages *in vitro* showing faster growth *in vivo*. Box plot representation of the results at day 11 (upper panels) and day 16 (lower panels). The middle line in each box plot is the median value, the upper and lower edges of the box plot are the 75th and 25th percentiles, and the small horizontal lines are placed at the observed value closest to 75th percentile and the 25th percentile plus 1.5 times the interquartile range. Significant reduction in tumor growth was observed only in thrombocytopenic tumor bearing-mice receiving chemotherapy (* $p \leq 0.05$; ** $p \leq 0.01$; ***$p \leq 0.001$).
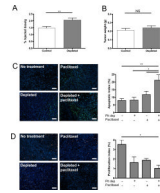
Figure 4. Thrombocytopenia increases paclitaxel delivery to mammary tumors and enhances its tumoricidal effects

Tumor-bearing mice were treated on day 10 with either a control IgG antibody (Control) or a platelet depleting antibody (Depleted), followed by the injection of ^{3}H-Paclitaxel. Two hours after the injection of the radio-labeled drug, the mice were sacrificed and the tumors harvested. A, Quantification of radioactivity in the tumor reported as percentage of injected dose per gram. B, Comparison of tumor weight between thrombocytopenic and control mice. (n=7-8 mice per group; * $p \leq 0.05$, $p > 0.05$; NS). C, Apoptosis staining using TUNEL labeling and quantification of apoptotic index on the tumors 72 hours post-treatment of tumor-bearing mice with either the IgG control or depleting antibody (Depleted) and paclitaxel or vehicle (No treatment). D, Proliferation staining using Ki-67 antibody and quantification of proliferation index. Original magnification 100X, Bar = 100μm. The apoptotic and proliferative indexes were calculated as the percentage of antigen positive-nuclei relative to Hoechst-stained nuclei. Mean of 8 microscopic fields of each tumor are represented (n= 4 tumors per group; * $p \leq 0.05$, **$p \leq 0.01$).
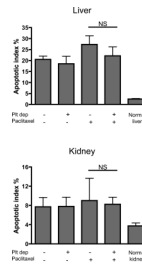
Figure 5. Thrombocytopenia in combination with paclitaxel does not increase apoptosis in the liver and kidney

72 hours post-treatment (as indicated) tumor-bearing mice were sacrificed and the liver and kidney were harvested and stained for TUNEL. The apoptotic index was calculated as the percentage of TUNEL-positive nuclei relative to Hoechst-stained nuclei. Platelet depletion in combination with paclitaxel treatment did not significantly affect apoptosis as compared to paclitaxel treatment alone. Mean of 8 microscopic fields of each organ are represented (n= 4 mice per group; $p > 0.05$; NS).
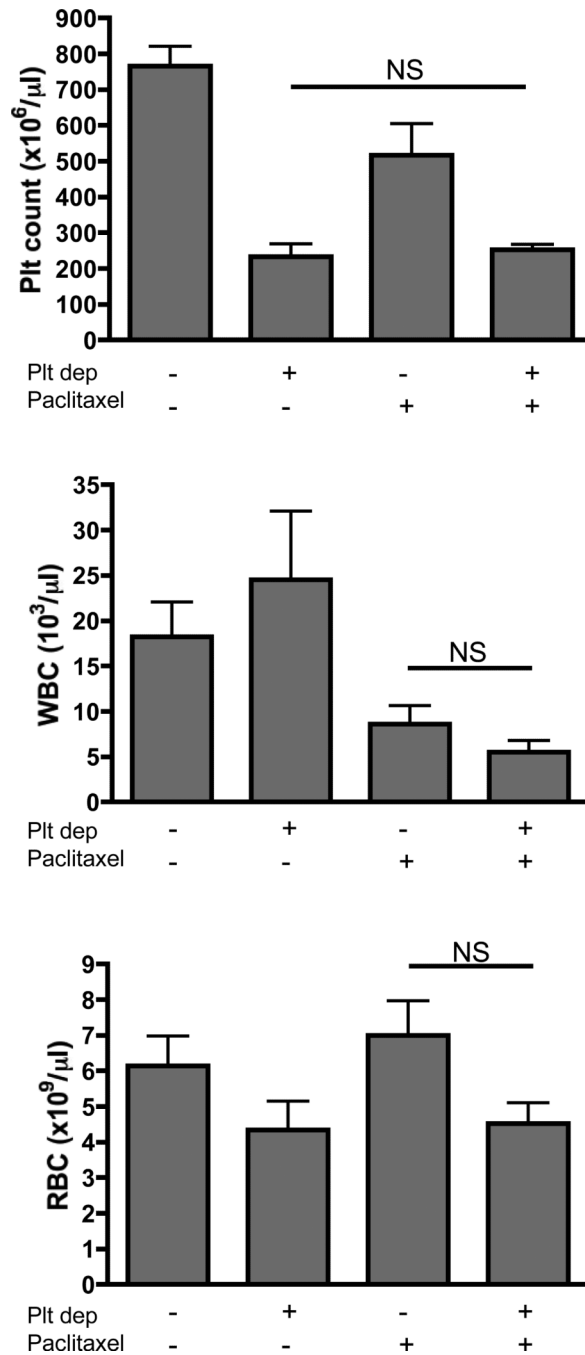
Figure 6. Thrombocytopenia in combination with paclitaxel does not increase side effects on blood cells counts

72 hours post-treatment (as indicated) blood of tumor-bearing mice was analyzed. Platelet, white blood cell and red blood cell counts are shown. In all cases, platelet depletion in combination with paclitaxel treatment did not significantly affect blood cell counts as compared to paclitaxel treatment alone (n=6-9 mice per group; $p > 0.05$; NS).
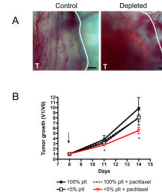
Figure 7. Thrombocytopenia favors the accumulation of microspheres and increases the efficacy of paclitaxel on LLC tumor growth

A, Dorsal skinfold chambers were surgically implanted on the backs of C57BL/6 mice. Two days later, LLC tumor cells were injected within skinfold chamber and allowed to grow. At day 5, mice were treated with either a control antibody (Control) or a platelet depleting antibody (Depleted) and 100×10^6 1μm fluorescent microspheres. Photographs of a control and a thrombocytopenic tumor were taken at 24 hours after platelet depletion. Original magnification 40X, Bar = 200μm. Results are representative of 3 different hemorrhagic tumors and nonhemorrhagic tumors. B, LLC tumor-bearing mice were treated on day 8 (arrow) as indicated and tumor growth was monitored. Tumor growth is represented as the ratio of the tumor volume at a specific day (V1) to the tumor volume before treatment (V0). At day 11 and 14, a significant reduction in tumor growth was observed in thrombocytopenic tumor bearing-mice receiving chemotherapy compared to mice with normal platelet count treated with paclitaxel alone (n=8-9 mice per group; * p ≤ 0.05).